JRA4

Final report on ^{195}Pt-NMR thermometer for ultra low temperatures
Reporting Period: **from 1.4.2009 to 30.9.2013**
Delivery dates: month 18, month 36
Lead beneficiary: **PTB**

Abstract. Both nuclear spin cooling and Pt-NMR thermometry are two parts of one and the same thermodynamic process. It arises from the solution of thermodynamic field equations for boundary and initial values that can be controlled in the process of nuclear cooling and pulsed NMR on high-purity bulk platinum samples, respectively. The temperature measured down to 10 μK agrees with that calculated by numerical solution of thermodynamic field equations with an uncertainty below 5% in the whole investigated temperature range from 10 μK to 10 mK.

1. Introduction

Pulsed nuclear magnetic resonance (NMR) on platinum is the only established method available at present for thermometry below 1 mK [1-3]. It consists of measuring the magnetisation of the nuclear spin system within a sample of metallic platinum, and relating it to temperature through the thermal state function. There are, however, a number of requirements which have to be complied with in order to obtain reliable results. All these requirements have been investigated systematically and form the main subject of a previous status report [4]. In continuation of the investigations on pulsed Pt-NMR thermometry at ultra-low temperature, the experimental platform of the PTB Mikrokelvin Facility in Berlin [5,6] has been improved by a platinum nuclear cooling stage for providing the direct measurement of the nuclear spin temperature T_N. The measurement of T_N by pulsed Pt-NMR is based on the spin dynamics described phenomenologically by a proper thermodynamic field theory. In order to test the thermodynamic consistency of the Pt-NMR thermometry, the measured temperature has to be compared to that determined by a proper thermodynamic field theory of nuclear spin cooling. That is the objective of the present final report.

2. Thermodynamic field theory

Thermodynamics of nuclear spin cooling is a field theory with the main objective to determine the nuclear spin temperature $T_N(\boldsymbol{x},t)$ and the conduction electron temperature $T_e(\boldsymbol{x},t)$ in all points $\boldsymbol{x}$ of a metal and at all times t. The required field equations can be derived from the kinetic theory of conduction electrons and nuclear spin relaxation.

If $f_e(\boldsymbol{x},\boldsymbol{p},m_s,t)\mathrm{d}^3x\mathrm{d}^3p$ denotes the number of free electrons in the phase space element $\mathrm{d}^3x\mathrm{d}^3p$ with z-spin $m_s \in [-\frac{1}{2},\frac{1}{2}]$, the phase density $f_e(\boldsymbol{x},\boldsymbol{p},m_s,t)$ will satisfy the Boltzmann transport equation

$$\frac{\partial f_{\mathrm{e}}}{\partial t}+\frac{p_i}{m_{\mathrm{e}}}\frac{\partial f_{\mathrm{e}}}{\partial x_i}+\dot{p}_i\frac{\partial f_{\mathrm{e}}}{\partial p_i}=S_{\mathrm{eN}}, \tag{1}$$

where S_{eN} is the collision term, which is primarily determined by Fermi contact interaction of the conduction electrons with the nuclei.

The state of the atomic nuclei in the metal is described by the probability density $w(\boldsymbol{x},m_{\mathrm{N}},t)$, whereby $w(\boldsymbol{x},m_{\mathrm{N}},t)\mathrm{d}^3x$ represents the probability to find a nucleus with *z*-spin $m_{\mathrm{N}}\in[-I,-I+1,....,I]$ in the volume element d^3x. The probability density obeys the Master equation

$$\frac{\partial w(\boldsymbol{x},m_{\mathrm{N}},t)}{\partial t}=S_{\mathrm{Ne}}(\boldsymbol{x},m_{\mathrm{N}},t), \tag{2}$$

with the production term $S_{\mathrm{Ne}}(\boldsymbol{x},m_{\mathrm{N}},t)$ resulting from the transition probabilities of nuclear spin states due to contact interaction with the conduction electrons.

Multiplication of the Boltzmann transport equation (1) by the energy of an electron $p^2/2m_{\mathrm{e}}+m_{\mathrm{s}}g_{\mathrm{s}}\mu_{\mathrm{B}}B$ in the magnetic field $\boldsymbol{B}(\boldsymbol{x},t)=(0,0,B(\boldsymbol{x},t))$, integration over the momentum space, and summation over the spin orientation quantum numbers m_{s} provide the energy balance of the electrons

$$\frac{\partial e_{\mathrm{e}}}{\partial t}+\frac{\partial q_i}{\partial x_i}=-n_{\mathrm{e}}\overline{\mu}_{\mathrm{e}}\frac{\partial B}{\partial t}+J_i\left(E_i+\frac{1}{e}\overline{\mu}_{\mathrm{e}}\frac{\partial B}{\partial x_i}\right)+P_{\mathrm{Ne}}+\dot{Q}_{\mathrm{ex}}. \tag{3}$$

Analogously, the energy balance of the nuclei can be derived by multiplying the Master equation (2) with the energy of a nuclear spin $-m_{\mathrm{N}}g_{\mathrm{N}}\mu_{\mathrm{n}}B$ in the magnetic field, and subsequent summation over the spin orientation quantum number m_{N}. For the energy balance of the nuclear spin system we get

$$\frac{\partial e_N}{\partial t}=-n_N\overline{\mu}_N\frac{\partial B}{\partial t}-P_{\mathrm{Ne}}. \tag{4}$$

$n_{\mathrm{N}}\overline{\mu}_{\mathrm{N}}$ and $n_{\mathrm{e}}\overline{\mu}_{\mathrm{e}}$ denote the products of the number densities of nuclear spins and conduction electrons and their average magnetic moments, respectively. q_i are the components of the energy flux, $\dot{Q}_{\mathrm{ex}}+\boldsymbol{J}\bullet(\boldsymbol{E}+\overline{\mu}_e/e\nabla\boldsymbol{B})$ is the heat leak density due to external sources and eddy currents, and P_{Ne} is the energy production density.

In order to obtain field equations, the energy balance equations (3) and (4) have to be supplemented by constitutive relations. For this purpose, we use the equations of state for a nuclear paramagnetic system and a strong degenerated electron gas. Then the average magnetic moments are given by the thermal state functions

$$\bar{\mu}_{\mathrm{N}} = g_{\mathrm{N}}\mu_{\mathrm{n}} I B_I(y), \qquad y = \frac{I g_{\mathrm{N}}\mu_{\mathrm{n}} B}{kT_{\mathrm{N}}} ,$$
$$\bar{\mu}_{\mathrm{e}} = \frac{3}{2}\frac{\mu_{\mathrm{B}}^2 B}{E_{\mathrm{F}}}\left(1-\frac{\pi^2}{12}\left(\frac{kT_{\mathrm{e}}}{E_{\mathrm{F}}}\right)^2\right), \tag{5}$$

where $\mathrm{B}_I(y)$ is the Brillouin function and E_{F} is the Fermi energy. The caloric state functions for the energy densities have the form

$$e_N = -n_{\mathrm{N}}\bar{\mu}_{\mathrm{N}} B ,$$
$$e_{\mathrm{e}} = n_{\mathrm{e}}\left[\frac{3}{5}E_{\mathrm{F}}\left(1+\frac{5\pi^2}{12}\left(\frac{kT_{\mathrm{e}}}{E_{\mathrm{F}}}\right)^2\right)-\bar{\mu}_{\mathrm{e}} B\right] . \tag{6}$$

The energy production density P_{Ne} is determined by hyperfine coupling of the conduction electrons with the nuclear spins involving a simultaneous electron-nuclear spin flip. It is given by

$$P_{\mathrm{Ne}} = -\frac{n_{\mathrm{N}} g_{\mathrm{N}}\mu_{\mathrm{n}} B T_{\mathrm{e}}}{2\kappa}\left[1-\left(\frac{\mu_{\mathrm{B}} B}{E_{\mathrm{F}}}\right)^2\right]\left[A_+\overline{m_N I_+}\exp\left(\frac{g_{\mathrm{N}}\mu_{\mathrm{n}} B}{kT_{\mathrm{e}}}\right)+A_-\overline{m_N I_-}\right] , \tag{7}$$

where

$$A_{\pm} = \exp\left[\pm\left(\frac{1}{kT_{\mathrm{N}}}-\frac{1}{kT_{\mathrm{e}}}\right)g_{\mathrm{N}}\mu_{\mathrm{n}} B\right]-1 . \tag{8}$$

κ is the Korringa constant and $\overline{m_N I_{\pm}}$ are combinations of Brillouin functions and their derivatives. From equation (7) it follows that the energy production density is approximately proportional to the electronic temperature T_{e}.

The components of the energy flux q_i appearing in equation (3) also constitute moments of the phase density $f_{\mathrm{e}}(\boldsymbol{x},\boldsymbol{p},m_{\mathrm{s}},t)$, viz.

$$q_i = \sum_{m_{\mathrm{s}}=-1/2}^{1/2}\int_{-\infty}^{\infty}\left(\frac{p^2}{2m_{\mathrm{e}}}+m_{\mathrm{s}} g_{\mathrm{s}}\mu_{\mathrm{B}} B\right)\frac{p_i}{m_{\mathrm{e}}} f_{\mathrm{e}}\mathrm{d}^3 p . \tag{9}$$

An energy flux balance following from the Boltzmann transport equation is obtained in the form

$$\frac{\partial q_i}{\partial t}+\frac{\partial N_{ij}}{\partial x_j} = \frac{J_i}{e}\bar{\mu}_{\mathrm{e}}\frac{\partial B}{\partial t}-\frac{\bar{\mu}_{\mathrm{e}}}{m_{\mathrm{e}}}P_{ij}\frac{\partial B}{\partial x_j}-\frac{e}{m_{\mathrm{e}}}E_j\left[P_{<ij>}+\frac{5}{3}\left(e_{\mathrm{e}}+\frac{2}{5}n_{\mathrm{e}}\bar{\mu}_{\mathrm{e}} B\right)\delta_{ij}\right]-\frac{e}{m_{\mathrm{e}}}(\boldsymbol{q}\times\boldsymbol{B})_i + S_i , \tag{10}$$

where the flux N_{ij} and the production S_i of the energy flux are given by

$$N_{ij} = \sum_{m_S=-1/2}^{1/2} \int_{-\infty}^{\infty} \left(\frac{p^2}{2m_e} + m_s g_s \mu_B B \right) \frac{p_i}{m_e} \frac{p_j}{m_e} f_e \mathrm{d}^3 p \quad , \tag{11}$$

$$S_i = \sum_{m_S=-1/2}^{1/2} \int_{-\infty}^{\infty} \left(\frac{p^2}{2m_e} + m_s g_s \mu_B B \right) \frac{p_i}{m_e} S_{eN} f_e \mathrm{d}^3 p \quad . \tag{12}$$

The momentum flux P_{ij} (pressure tensor) includes the electron energy density e_e, according to the decomposition

$$P_{ij} = \sum_{m_S=-1/2}^{1/2} \int_{-\infty}^{\infty} m_e \frac{p_i}{m_e} \frac{p_j}{m_e} f_e \mathrm{d}^3 p = P_{<ij>} + \frac{2}{3} \left(e_e + n_e \overline{\mu}_e B \right) \delta_{ij} \quad . \tag{13}$$

Insertion of the constitutive equations (5) to (13) into the energy balance equations (3) and (4) leads to a set of explicit field equations for both the nuclear spin temperature $T_N(\boldsymbol{x},t)$ und the electronic temperature $T_e(\boldsymbol{x},t)$. A solution of these field equations is called a thermodynamic process of nuclear spin cooling. Generally, thermodynamic processes of nuclear spin cooling are not continuous in space, because the magnetic flux density $B(\boldsymbol{x},t)$ exhibits a spatial variation. Consequently, the temperature fields $T_N(\boldsymbol{x},t)$ and $T_e(\boldsymbol{x},t)$ also show a spatial dependence. The evaluation of the thermodynamic process of nuclear spin cooling requires the numerical solution of partial differential equations for boundary and initial values that can be controlled in the nuclear demagnetisation experiment.

The measurement of temperature by use of pulsed nuclear magnetic resonance is a part of the thermodynamic process of nuclear spin cooling. It has to be kept in mind, however, that the magnetic flux density in the measuring region takes the form $\boldsymbol{B}(\boldsymbol{x},t) = (B_1(\boldsymbol{x})\cos(\omega_0 t), 0, B_0(\boldsymbol{x}))$. That means that in addition to the main field B_0, aligned parallel to z-axis, there is an oscillating field $B_1(\boldsymbol{x})$ at the Larmor frequency ω_0, produced by a small coil positioned along x-axis. Hence, the average magnetic moment $\overline{\boldsymbol{\mu}}_N$ is no longer described by the thermal state equation (5), and the field equations have to be extended. For that purpose the Master equation (2) is multiplied by the magnetic moment of a nucleus, which is proportional to its spin according to $\boldsymbol{\mu}_N = \gamma \cdot \boldsymbol{I}$. $\gamma = g_N e / 2m_p$ is the so-called gyromagnetic ratio. The subsequent summation over the spin quantum number m_N results in the Bloch equation

$$\frac{\partial M_i}{\partial t} - \gamma \varepsilon_{ijk} M_j B_k = \sum_{m_N=-I}^{I} \mu_i S_{Ne} \quad , \tag{14}$$

describing the dynamics of nuclear magnetisation. In the relaxation-time approximation, the production term on the right side of equation (14) can be expressed by

$$-\frac{(M_z - M_z^0)e_i^3}{\tau_1} - \frac{M_x e_i^1 + M_y e_i^2}{\tau_2} \quad . \tag{15}$$

$M_z^0 = n_N \bar{\mu}_N$ is the thermal equilibrium value of nuclear magnetisation in the presence of the main field B_0 only, which can be calculated from equation (5); τ_1 and τ_2 are time constants characterising the relaxation process of the nuclear spin system after it has been disturbed from its thermal equilibrium state by the action of the oscillating field $B_1(\boldsymbol{x})$. In order to describe pulsed nuclear magnetic resonance measurements including radiation-damping effects, the Bloch equations have to be combined with the Maxwell equations.

An analysis of the thermodynamic process of pulsed nuclear magnetic resonance thus requires the solution of the extended field equations. In the case of a cylindrical platinum rod, the amplitude of the oscillating excitation field $B_1(r)$ is reduced and the phase is shifted, when penetrating into the metallic sample as shown in Figure 1.

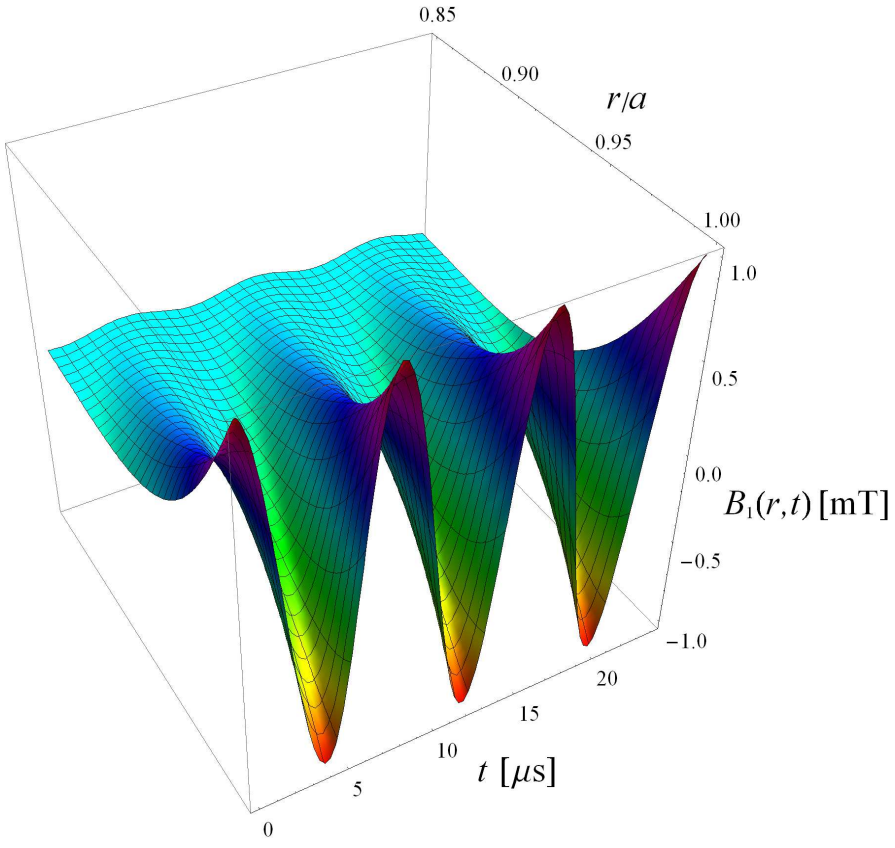

Fig. 1: The excitation field $B_1(r,t)$ perpendicular to the main field $B_0\boldsymbol{e}_3$ in a cylindrical platinum rod of radius a = 1.5 mm, as resulting from the solution of Maxwell's equations in matter for an electrical conductivity of $\sigma_{Pt} = 5.28 \cdot 10^8\ \Omega^{-1}\mathrm{m}^{-1}$. The excitation field oscillating at 125 kHz is turned on for 24 μs.

The magnetic field produced by both the demagnetisation magnet and the NMR magnet system determines the thermodynamic process of nuclear spin cooling as well as the temperature measurement by pulsed nuclear magnetic resonance.

3. Experimental set-up

In continuation of previous investigations on pulsed platinum NMR thermometry at ultra-low temperature, the experimental platform of the microkelvin cryostat (MKA3) has been improved by a platinum nuclear cooling stage providing the direct measurement of the nuclear spin temperature. The double-stage setup of the nuclear cooling facility is pictured in Figure 2.

Fig. 2 : Double-stage setup of the nuclear cooling facility, consisting of the (*top*) main copper stage, the (*lower*) central platinum stage enclosed by an aluminium cylinder stage, and the (*intermediate*) heat switch.

The main nuclear cooling stage consists of a cylindrical copper tube with a length of 350 mm, an outer diameter of 116 mm, and an inner diameter of 100 mm. Eighty vertical slits are placed along a length of 309 mm to reduce eddy current heating during demagnetisation. The total mass of the main stage is 6.67 kg (105 moles copper). Taking into account the variation of the magnetic field B_0 over the length of the stage (as illustrated in Fig. 3), the effective amount of copper in the field is equivalent to 4.15 kg (65.3 moles copper). On the top flange both the superconducting heat switch and the mechanical attachment connect the nuclear cooling stage with the mixing chamber sample holder of the dilution refrigerator. The superconducting heat switch consists of thirty highly pure aluminium foils with a thickness of 0.1 mm, and the mechanical attachment is realised by three Vespel tubes of 150 mm length.

A second heat switch, consisting of twelve 0.1 mm thick aluminium foils, controls the thermal connection between the main nuclear cooling stage and the lower cooling stage unit. It is located in the field-compensated region between both stages, and attached to two copper plates that are spaced by three Vespel tubes of 80 mm length. The thermal and mechanical connection to the upper and lower cooling stages is realised by three hollow rods of copper with lengths of 130 mm and 250 mm, respectively.

The lower cooling stage unit is composed of a central platinum stage and an enclosed aluminium cylinder stage with a mass of 55.84 g (2.07 mole aluminium). The mass of the platinum stage is 291.75 g (1.5 mole platinum), in which the natural abundance of the only magnetic isotope ^{195}Pt is 33.8%. Both stages are connected by niobium threaded pins acting in the field of demagnetisation as intrinsic heat switch. If the magnetic flux density during demagnetisation reaches values below the critical field of niobium (B_c = 200 mT), the nuclear stages thermally decouple from each other. Similarly, the aluminium stage becomes superconducting when the applied field is further reduced below the critical field of aluminium (B_c = 10.5 mT).

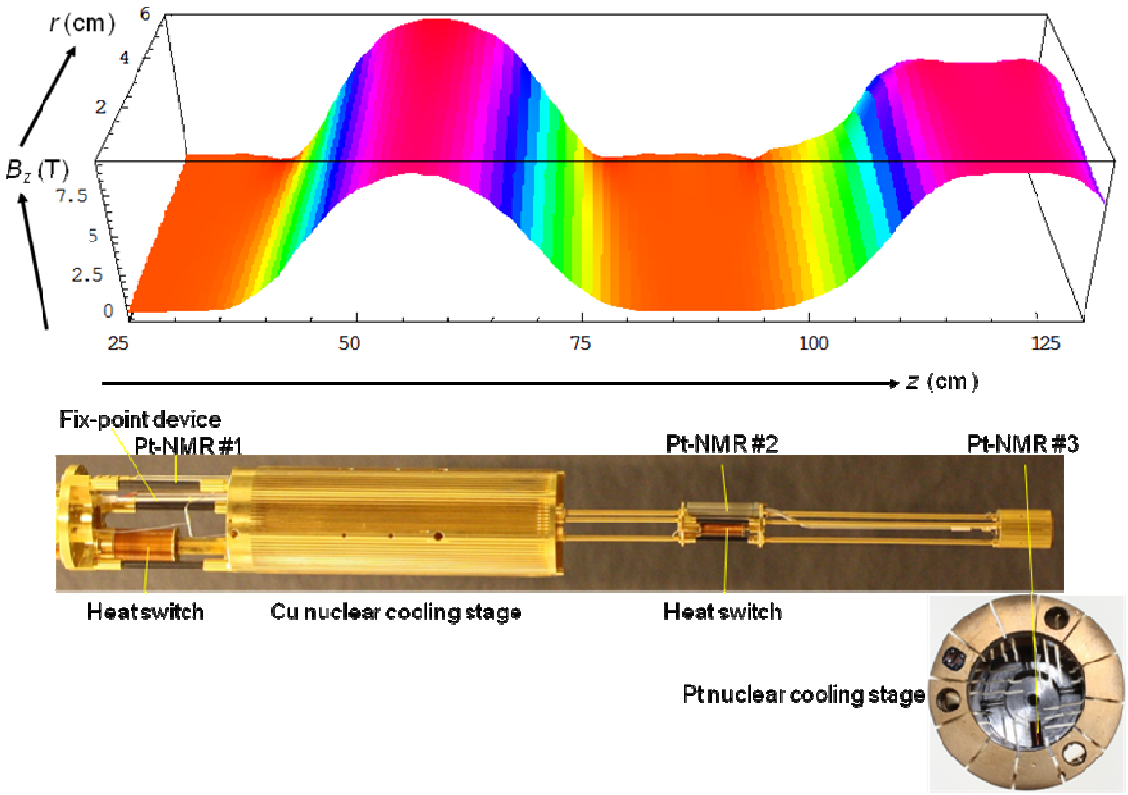

Fig. 3 : (*top*) Magnetic field profile generated by the two-stage superconducting magnet of the microkelvin cryostat MKA3. (*bottom*) The photo of the double-stage setup indicates the positions of the nuclear cooling stages and the Pt-NMR thermometers in the magnetic field.

To measure the temperature by means of pulsed platinum nuclear magnetic resonance (Pt-NMR), three bulk platinum thermometers have been installed (as indicated in Fig. 3). They have been tested on the double-stage setup of the nuclear cooling facility. The thermometer Pt-NMR #1 is located in a field compensated region of the superconducting magnet to measure the electronic temperature T_e on top of the copper nuclear cooling stage. A high purity platinum rod of 4 mm diameter is used to measure the electronic temperature of the platinum nuclear stage in a field compensated region. For this purpose, the bottom end of the platinum rod is screwed into the central bore hole of the platinum stage, and at the other end the thermometer Pt-NMR #2 is attached. Ultimately, the thermometer Pt-NMR #3 is a cylindrically shaped part of the platinum nuclear cooling stage itself, as visible in the photo of Fig. 3. This thermometer thus permits to measure the nuclear spin temperature T_N of the platinum stage in the final magnetic field.

The measurement of both the nuclear spin temperature and the electronic temperature is based on the thermodynamic process of pulsed NMR in a cylindrical platinum sample that results from the solution of extended field equations. In order to test the thermodynamic consistency of the pulsed Pt-NMR thermometry, the measured temperature has to be compared to that determined by evaluation of the thermodynamic process of nuclear spin cooling.

4. Testing of the pulsed Pt-NMR thermometry down to 10 μK

Figure 4 gives an example of a typical nuclear free precession signal from a cylindrical bulk platinum sample at 79 μK and in a steady magnetic field B_0 = 14.2 mT.

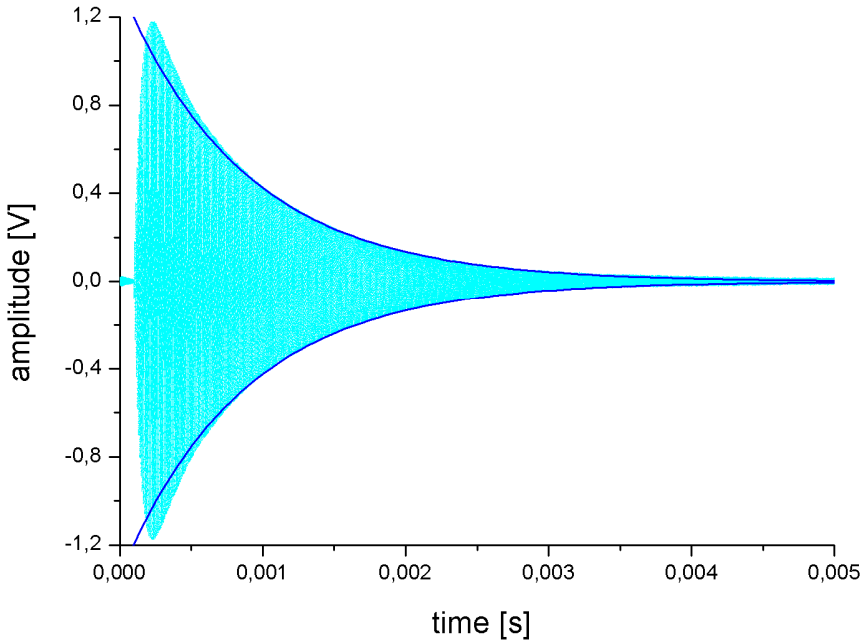

Fig. 4 : A 10 MHz sampled record of a 125 kHz bulk platinum FID at 79 μK in a steady magnetic field B_0 = 14.2 mT. The blue lines represent the exponential decay of the FID.

The FID signal amplitude is a distorted form of $U(t) \propto M_0 f(\vartheta)\omega \sin(\omega t + \varphi)\exp(-t/\tau_2)$, where $\omega = \gamma B_0$. Distortion is due to residues of the transmitter burst and transients from the protective preamplifier gates. In addition, the signal contains also some ringing after transmission of the transmitter pulse (as seen in Fig. 4). Therefore, only data recorded after all initial transients have died out ($t \gtrsim 800$ μs) are analysed. A signal fitting analysis results in the determination of the signal amplitude ($U(0)$ = (1.40096 ± 0.00052) V), the frequency (ω/2π = 124.04470 ± 0.0754) kHz), the phase (φ = 0.30352 ± 0.0001197), and the spin-spin relaxation time ($\tau_2 = (0.8463 \pm 0.000199)$ ms). The FID signal amplitude function $U(t)$ fits the recorded data very well, with a mean deviation $\chi^2_{\text{red}} = 6.9619 \times 10^{-6}$ and an adjusted coefficient of determination $\overline{R}^2 = 0.99979$. Figure 5 shows both the 10 MHz sampled record of the bulk platinum FID for 1.0 ms ≤ t ≤ 1.4 ms and the fitted FID signal amplitude function.

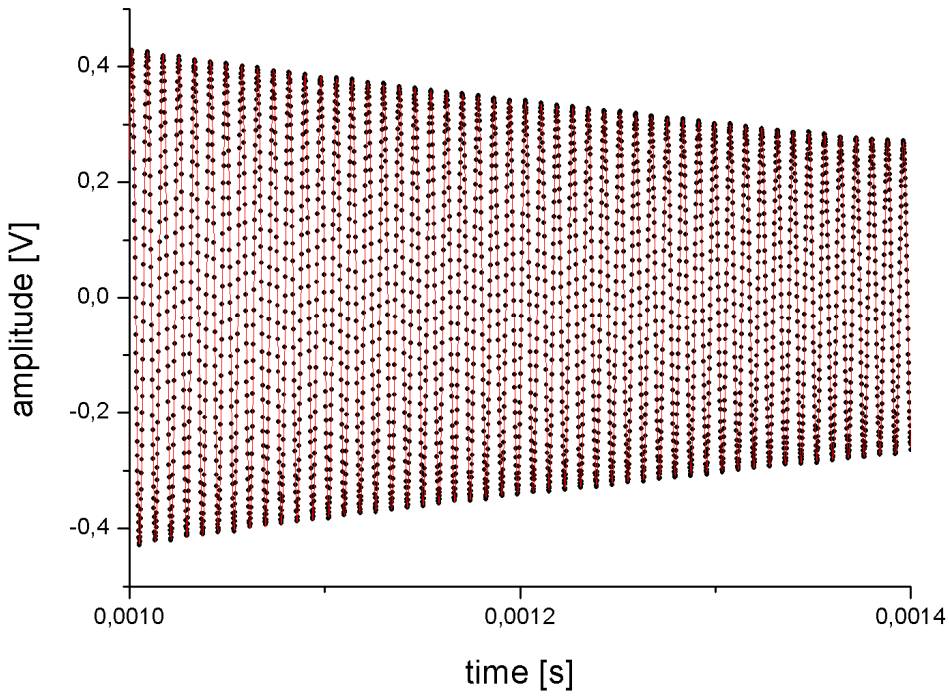

Fig. 5 : The 10 MHz sampled record of a bulk platinum FID already displayed in Fig. 4 is here shown in the time range from 1 ms to 1.4 ms (black dots). The red graph represents the fitted FID signal amplitude.

The evaluated FID signal amplitude $U(0)$ is proportional to the magnetisation M_0. On basis of the thermal equation of state $M_0(B_0,T_N)$ according to Eq. (5), the temperature was determined to be T_{NMR} = 79 μK. The measured temperature is then compared to that calculated from the thermodynamic field theory. A temperature T = 78.3 μK was obtained by numerical solution of the thermodynamic field equations. This temperature

corresponds to both the electronic temperature T_e and the nuclear temperature T_N in the bulk platinum thermometer at time just before the onset of the RF pulse. The relative deviation of measured temperature from thermodynamic temperature seems to be small ($(T_{NMR}-T)/T = 0.89\%$). It is plotted in Figure 6, together with results obtained in another nuclear cooling experiment [4].

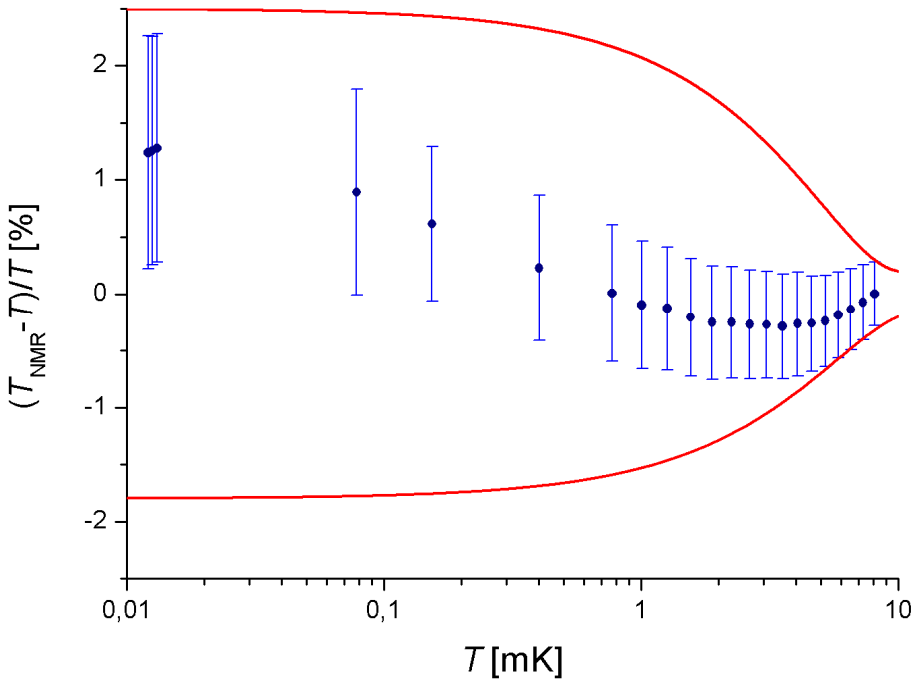

Fig. 6 : Relative deviation of measured magnetic temperature T_{NMR} from thermodynamic temperature T in a temperature range from 10 μK to 10 mK (blue dots). Error bars denote statistical and systematic uncertainties of measurements. The red solid lines mark the thermodynamic uncertainty of the platinum NMR-based thermometry.

The statistical and systematic uncertainties (added in quadrature) of the pulsed platinum NMR were determined from replicate measurements. Thereby, the systematic uncertainties are mainly due to calibration of the Pt-NMR thermometer at temperatures above 15 mK.

Although the relative deviation (T_{NMR}-T)/T is small over three decades of temperature, it is systematic and increases to lower temperature. This is caused by the uncertainty of thermodynamic field theory, which is based on the kinetic theory of degenerate non-relativistic electron gas and nuclear spin relaxation. In order to improve the thermodynamic field theory, both electron and nuclear spin correlations (for platinum in particular) have to be considered. In fact, the observed systematic deviation of the measured magnetic temperature from the thermodynamic temperature can be considerably reduced by introducing an effective electron mass. Another adjustable parameter includes various heat leaks in nuclear refrigeration. Even though adjustable

parameters can be found that most closely match the magnetic temperatures measured in nuclear cooling experiments, they must be determined otherwise (e.g. susceptibility measurements). This was done in order to estimate approximately the thermodynamic uncertainty of the platinum NMR-based thermometry, which is visualised in Figure 6.

Preliminary results of nuclear spin temperature measurement on the platinum nuclear stage confirm its thermodynamic consistency. The relative deviation of the measured nuclear spin temperature from the calculated thermodynamic temperature T_N exhibits a more distinct characteristic temperature dependence than that found in nuclear refrigeration of copper. This is due to the electron configuration in platinum metal. The thermodynamic uncertainty of the platinum NMR-based thermometry, however, has been estimated to be below 5% (as marked in Fig. 6).

5. Conclusion

Pulsed Pt-NMR on high-purity bulk samples has been used to measure temperatures down to 10 μK. The measured temperature agrees with that calculated by numerical solution of thermodynamic field equations for given boundary and initial values of a nuclear demagnetisation process with an uncertainty below 5% in the whole investigated temperature range from 10 μK to 10 mK. Thus the NMR-based temperature scale [7] has been extended to three orders of magnitude. In order to establish this ultra-low temperature scale, both a comparison of the Pt-NMR thermometer with primary thermometers (such as noise thermometer) and a dissemination of the scale using superconducting fixed points have to be realised.

References

[1] O. Lounasmaa, “Experimental Principles and Methods Below 1 K”, Academic Press London (1974)
[2] F. Pobell, “Matter and Methods at Low Temperatures”, Springer-Verlag, Berlin Heidelberg (1992)
[3] E. Fukushima and S. Roeder, “Experimental Pulse NMR”, Addison-Wesley, New York (1981)
[4] ^{195}Pt-NMR thermometer for ultra low temperature, Internal Report Deliverable D6, European Microkelvin Collaboration, (2010)
[5] P. Strehlow, H. Nuzha, and E. Bork, “Construction of a Nuclear Cooling Stage”, J. Low Temp. Phys. **147**, 81 (2007)
[6] P. Strehlow, “Optimized Thermodynamic Process of Nuclear Cooling”, AIP Conf. Proc. **850,** LT 24, 1575 (2006)
[7] D. Hechtfischer, and G. Schuster, “The Quality of the Curie Law in Platinum-NMR” in : Temperature: Its Measurement and Control in Science and Industry, Vol. **7**, edited by D. Ripple, AIP, New York, 47 (2003)